

A Method for Measuring Lateral Electrical Field Effects within CCDs

Distinguishing between quantum efficiency and charge transport anomalies

Christopher W. Stubbs

Received: date / Accepted: date

Abstract Improving the precision of astronomical measurements requires careful attention to all aspects of system performance. Dark energy science demands improved precision, as do radial velocity and extrasolar transit measurements. Under uniform illumination CCDs do not produce a uniform distribution of flux in the detector pixels. This variation has historically been attributed to spatial variations in quantum efficiency (QE). But recent experience has shown that much (and perhaps most) of the high spatial frequency variation comes about due to lateral electrical fields within the silicon that produce charge transport anomalies. These lateral field effects are more pronounced in deep depletion detectors, but are nevertheless apparent in data taken with more conventional devices. A major measurement challenge is distinguishing genuine quantum efficiency variations from these charge transport anomalies. This paper describes a technique that (at least in principle) should allow for the discrimination between lateral electrical fields and QE on the lab bench, potentially leading to a method of more precise flat-fielding of CCD data for both imaging and spectroscopic applications. The essence of the technique is to use carefully controlled gradients in surface brightness to map out the electrical field distribution in the array.

Keywords Astronomical Instrumentation · CCDs · precision calibration · LSST

PACS 95.55.Aq · 95.55.Qf · 95.75.De

Christopher W. Stubbs
Department of Physics & Department of Astronomy
Harvard University
17 Oxford Street
Cambridge MA USA 02138
Tel.: +1-617-495-1454
E-mail: stubbs@physics.harvard.edu

1 Introduction

1.1 Early work

Mark Downing, Roger Smith, HST stuff too

1.2 Contemporary Astronomical CCDs, and Gremlins therein

2 Lateral Electric Fields in CCDs, Charge Transport, and Improper Flat-Fielding

Figure 1 shows how lateral electric fields around the periphery of a pixel can generate charge transport anomalies. As photocharge is moved in the z direction (normal to the plane of the detector) any lateral \mathbf{E} fields will determine where it actually ends up. These lateral electric fields can arise in a variety of ways, including impurities in the silicon crystal from which the detector was fabricated, fields due to accumulated photo-charge in the arrays, guard ring and other electrode structures in the device, and meandering channel stops. The papers from the Nov 2013 workshop on “Precision Astronomy with Deeply Depleted CCDs” has multiple papers (cite them) that describe these effects.

2.1 Evidence of Detector Artifacts from PanSTARRS, Dark Energy Survey, HSC, and LSST Prototype Sensors

There is now ample evidence of lateral electric fields producing undesirable artifacts in CCD images. The Dark Energy Camera shows evidence (cite) for astrometric distortions on small scales that are correlate with ring-like structures seen in the flatfields. This is attributed to (right words) tree rings. The LSST prototype detectors show a distorted response function (cite) under flat illumination that is not seen in aperture photometry of point sources, that influences photometry and astrometry as far as 10 pixels from the edges of the devices. The PanSTARRS team has reported (cite Mangier) correlations between astrometric residuals, photometric residuals, and features seen in their flatfield data. The Hyper-Suprime-Cam team has also reported (cite BNL talk) similar features in their images.

2.2 The Measurement Challenge: Distinguishing QE variations from charge transport effects

The measurement challenge is to devise one or more schemes to distinguish between genuine QE variations (differences in the likelihood of an incident photon producing an electron) and charge transport effects, that can produce short-range variations of flux between adjacent pixels, that can therefore masquerade as QE variations. Mis-interpretation of these flux variations leads to

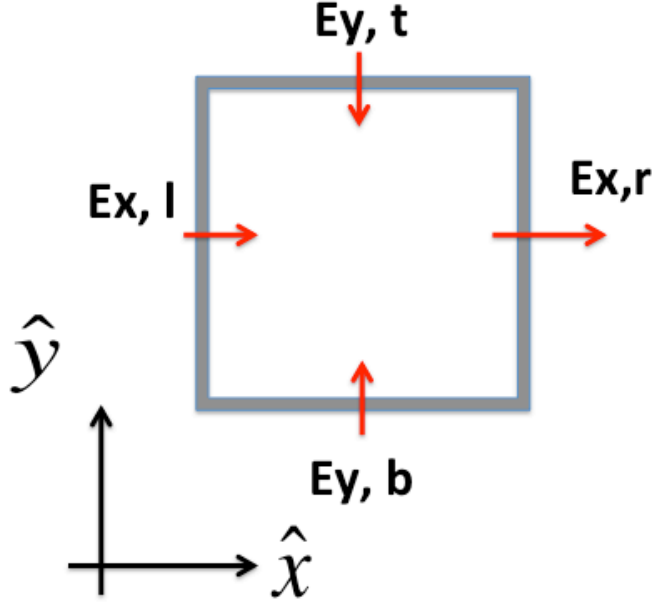


Fig. 1 Lateral electrical field distribution around the boundary of a pixel. The E_x components determine charge transport from the vertical edges, while the E_y components determine the charge leakage across the horizontal edges. The surface brightness ϕ also plays a role. The difference of the product $\phi_L E_{x,L} - \phi_R E_{x,R}$ determines the net leakage in the horizontal direction, and an analogous term governs the net excess charge following into the pixel across the horizontal boundaries. In this example $E_{y,t}$ is a negative number, and the other edge field components are positive numbers.

the construction of inappropriate flat fields, and we introduce systematic errors that are in principle avoidable, but only if we can identify the true variable-QE component.

We'd also like to correct for the charge transport effects, which produce systematic errors in astrometry, photometry, and shape measurements.

For the purpose of this paper we will make the following assumptions:

- The horizontal transport of charge across pixel boundaries can be considered as arising from an effective horizontal component $\mathbf{E}_{\text{horiz}}$ of electric field.
- The amount of charge that moves across a pixel boundary depends on the product of the local surface brightness $\phi(x, y)$ times the component of the horizontal field that is normal to the boundary.

- We will assume that the pixel lithography is perfect, with no mask step-repeat errors.
- We will suppress any wavelength dependence of the effective electric field strength, although the test described here could be carried out at various wavelengths to map out the effective lateral field strength as a function of wavelength.
- We will ignore the influence of accumulated charge in the pixels, and will assume the lateral E fields are frozen in place and are static.
- The treatment here assumes the CCD is accumulating electrons, not holes.
- We will ignore (at least initially) any QE variations in the device.

3 Arithmetic for Tracking the Charge Transport between Pixels

Under the assumptions listed above, we consider the charge transport anomalies arising from the combined effect of the incident flux $\phi(x, y)$ and the horizontal electric field $\mathbf{E}(x, y)$. We define four components of the electric field normal to the four pixel edges (really the average along the appropriate pixel edge). The edges are labelled as *left*, *right*, *top* and *bottom*. The horizontal electric field and flux landing on the center of each pixel will be designed with integer indices; $\phi(i, j)$ and $\mathbf{E}(i, j)$. The field components of interest along the pixel edges are $E_{x,l}$, $E_{x,r}$, $E_{y,t}$ and $E_{y,b}$ where the \hat{x} and \hat{y} directions are defined in Figure 1 and l, r, t, b represent left, right, top and bottom edges respectively. We'll also want to define ϕ_l, ϕ_r, ϕ_t and ϕ_b , the photon fluxes (manifestly positive quantities) that land on these edges.

Assuming the CCD is accumulating electrons and not holes, a positive $E_{x,l}$ (electric field component pointing from the left edge towards the pixel center) pulls charge out of the pixel. Assuming that the flow at each edge is governed by the product of the surface brightness ϕ times the appropriate E-field component, we can write down the various amount of charge that crosses the borders. We will adopt a sign convention that positive transport brings charge into the pixel. The net charge $\Delta(i, j)$ that flows into the pixel due to horizontal fields and illumination intensity is then the sum of these four terms;

$$\begin{aligned}
 \text{L: charge in from the left edge } \Delta L &\propto \phi_l \times -E_{x,l}. \\
 \text{R: charge in from right edge } \Delta R &\propto \phi_r \times E_{x,r}. \\
 \text{T: charge in from top edge } \Delta T &\propto \phi_t \times E_{y,t}. \\
 \text{B: charge in from bottom edge } \Delta B &\propto \phi_b \times -E_{y,b}.
 \end{aligned}
 \tag{1}$$

Now we can use Taylor series expansions to relate the E-fields and photon fluxes at the edges of the pixel to the values $\phi(i, j)$ and $\mathbf{E}(i, j)$ at the center of the pixel. Taking s to be the side length (common to the x and y directions) gives $\phi_l = \phi(i, j) + \frac{d\phi}{dx}(-s/2)$; $E_{x,l} = E_x(i, j) + \frac{dE_x}{dx}(-s/2)$, etc. Retaining

only first order contributions, after collecting terms we arrive at a pleasantly symmetrical expression;

$$\Delta(i, j) = \alpha \left[\phi(i, j) \left[\frac{dE_x}{dx}(s) + \frac{dE_y}{dy}(s) \right] + E_x(i, j) \frac{d\phi}{dx}(s) + E_y(i, j) \frac{d\phi}{dy}(s) \right], \quad (2)$$

where α is a constant of proportionality, assumed equal on all edges.

We have no direct control over the E-field terms in equation (2), but we can impose structured illumination that has different intensities and spatial gradients. Illumination with light that has a gradient in only the x direction can be used to determine the value of $E_x(i, j)$; it's the coefficient of $\Delta(i, j)$ that depends on the x component of the illumination gradient, if the average illumination level $\phi(i, j)$ is kept constant. Similarly we can measure $E_y(i, j)$ as the coefficient of the y component of the illumination gradient.

The main point of this paper is that a judicious combination of uniform illumination levels and imposed illumination gradients in the x and y directions can be used in conjunction with equation (2) to map out the lateral electrical fields $E_{x,y}(i, j)$ across the CCD array. With these numbers in hand we can readily interpolate to determine the values of E_x and E_y at the boundaries between pixels, and the expressions in equation (1) could be then used to (in conjunction with the measurement of $\phi(i, j)$ and its gradients, in each image) to determine the corrections needed to account for the flux sharing between any pixel and its four neighbors.

3.1 A Possible Consistency Check Exploiting $\nabla \times \mathbf{E} = 0$.

My thanks to Robert Lupton for pointing out the fact that the lateral E field must be curl-free. This allows for a powerful consistency check and assessment of uncertainties. Note that the E-field is in general not divergence free, since the impurities do introduce a non-zero charge imbalance in the lattice.

4 Laboratory Measurement Opportunities

The ideal situation would be to project onto the CCD a clean pattern that produces a uniform gradient in the x or y directions. This can be accomplished in a variety of ways, including using interference between two coherent beams, projecting a sinusoidal MTF test pattern onto the device, or projecting a slightly out of focus image of a transmission grating with uniform backlighting (such as from an integrating sphere's output port). A high-contrast one-dimensional periodic pattern with a wavelength of a few pixels seems ideal, at first blush. Shifting this along the array in the direction that has the gradient would allow us to test the recovered E-field with a sign flip in the gradient and different mean flux levels.

5 On-Sky Measurement Opportunities

6 Conclusions